JCC Plus

WILEY

ORIGINAL ARTICLE OPEN ACCESS

Altered Levels of Enteric Glial Cells and Their Associated Pro-Inflammatory Proteins in Patients With Ulcerative Colitis During Active Disease Compared to Remission and Healthy Controls

Julie Beaudeau[1] | Georgios Katinios[2,3] | Carl Mårten Lindqvist[4] | Susanna A. Walter[2,3] | Simone Ignatova[5] | Olga Bednarska[2,3] | Andreas Münch[2,3] | Johan D. Söderholm[1] | Jonas Halfvarson[6] | Benita Salomon[4] | Ida Schoultz[4] | Henrik Hjortswang[2,3] | Åsa V. Keita[1]

[1]Department of Biomedical and Clinical Sciences, Linköping University, Linköping, Sweden | [2]Department of Health, Medicine and Caring Sciences, Linköping University, Linköping, Sweden | [3]Department of Gastroenterology and Hepatology, Linköping University, Linköping, Sweden | [4]School of Medical Sciences, Faculty of Medicine and Health, Örebro University, Örebro, Sweden | [5]Department of Clinical Pathology and Clinical Genetics, Linköping University, Linköping, Sweden | [6]Department of Gastroenterology, Faculty of Medicine and Health, Örebro University, Örebro, Sweden

Correspondence: Åsa V. Keita (asa.keita@liu.se)

Received: 2 December 2025 | **Revised:** 15 January 2026 | **Accepted:** 21 January 2026

Keywords: enteric nervous system | gut inflammation | immunofluorescence | inflammatory bowel disease

ABSTRACT

Background: Enteric glial cells (EGC) play a crucial role in gut barrier maintenance but their role in ulcerative colitis (UC)-related inflammation is largely unknown. This study investigated EGC and related proteins in patients with UC in inflamed and non-inflamed segments during clinically active disease and remission following anti-inflammatory treatment.

Methods: Colorectal biopsies were obtained from inflamed and non-inflamed segments of 14 patients with UC before and after initiating anti-inflammatory therapy and achieving clinical and endoscopic remission. Control biopsies were collected from 16 healthy controls (HC). EGC markers: glial fibrillary acidic protein ($GFAP^+$) and S100 calcium-binding protein β ($S100\beta^+$) were assessed by immunofluorescence. Relative estimates of inflammatory proteins in biopsies were analyzed using Olink technology. The EGC cell line CRL-2690 was exposed to interleukins (IL)-4 and IL-6 at varying concentrations and durations, and analyzed by western blotting.

Results: EGC^{GFAP+} and $EGC^{S100\beta+}$ were more abundant in inflamed colonic segments during active UC compared to remission ($p < 0.001$) and HC ($p < 0.0001$). In non-inflamed segments, EGC^{GFAP+} decreased significantly with remission ($p < 0.001$), whereas $EGC^{S100\beta+}$ remained stable. Interleukin stimulation modulated GFAP expression in vitro, with IL-6 increasing and IL-4 decreasing in a dose and time-dependent manner. EGC-associated proteins, including cytokines, neurotrophic factors and chemokines were elevated in inflamed segments during active UC, normalizing towards HC levels upon remission.

Conclusion: Elevated EGC counts, and associated pro-inflammatory proteins characterize inflamed mucosa during clinical active UC. These novel findings suggest that EGC may be clinically relevant for identifying novel biomarkers for disease monitoring.

Plain Language Summary

Ulcerative colitis (UC) is a chronic intestinal disease where the lining of the colon and rectum is chronically inflamed, but the role of enteric glial cells (EGC) in the inflammatory process, is not well understood. In this study, we examined tissue samples

from 14 patients with UC during active disease and after anti-inflammatory treatment from the inflamed and non-inflamed part of the colon, as well as from healthy controls. We focused on two proteins markers of EGC and measured EGC inflammation-related proteins. We found that EGC were much more abundant in inflamed tissue during active UC compared to tissue in remission or from healthy controls. In non-inflamed tissues, one EGC marker decreased after treatment, whereas the other stayed stable. In addition, our study shows that specific immune signals (interleukins) could change the activity of EGC, with IL-6 increasing and IL-4 decreasing levels of one marker. Overall, inflamed tissue in UC showed higher levels of EGC and related inflammatory proteins, which returned closer to healthy controls after treatment. These findings suggest that EGC are closely linked to inflammation in UC and could potentially serve as useful biomarkers to monitor disease activity and treatment response.

1 | Introduction

Ulcerative colitis (UC), one major subtype of inflammatory bowel disease (IBD), is an immune-mediated disorder characterized by chronic mucosal inflammation of the colon and rectum. The disease typically progresses through relapses, alternating between episodes of active inflammation and periods of remission, during which there is no disease activity. During flares patients often experience symptoms of bloody diarrhea, abdominal pain and cramping [1, 2].

Although the exact pathophysiology of UC remains unclear, evidence suggests that chronic intestinal inflammation can cause structural and functional changes within the enteric nervous system (ENS) [3]. Enteric glial cells (EGC) are non-neuronal cells of the ENS that play a crucial role in maintaining gut barrier homeostasis by secreting factors, such as cytokines and neurotrophic factors [4, 5]. Notably, they constitute a heterogeneous population, distinguished by the expression of various markers including glial fibrillary acidic protein (GFAP), S100 calcium-binding protein β (S100β), proteolipid protein 1 (PLP1), and transcription factor Sox10 [4]. Patients with IBD display defects in EGC networks [6] and their reactions, characterized by phenotypic and functional alteration may contribute to inflammation, a dysfunctional intestinal barrier [6–8], and impaired neuronal integrity [9].

We recently demonstrated an increased number of EGC in the ileal mucosa of patients with Crohn's disease (CD), another subtype of IBD [10], by examining the two markers GFAP and S100β. These findings align with previous research indicating an increased expression of EGC markers in inflamed segments of patients with active IBD compared to healthy controls (HC) [11–13], suggesting increased activation and a potential role in amplifying inflammatory response [14, 15]. Therefore, understanding the role of EGC in inflammatory conditions following disease state, along with the dynamic interplay between EGC activation and enteric neuronal function is crucial for advancing our knowledge of UC-related inflammation.

Based on these considerations, we aimed to study the involvement of EGC in both clinically active and quiescent UC. We examined the characteristics of EGC and their associated proteins by analyzing inflamed and non-inflamed biopsies from patients with clinically active UC initiating anti-inflammatory therapy and from the same patients and biopsy locations after achieving clinical and endoscopic remission. Additionally, we compared the results to biopsies obtained from HC.

2 | Materials and Methods

2.1 | Patient Cohort and Ethical Considerations

Patients (8 men and 6 women, median age 38.5 years [range 21–72 years]) with known UC were included in the study (Table 1). Prior to initiating anti-inflammatory treatment, a flexible sigmoidoscopy was performed after bowel preparation with a rectal enema. The study was performed in accordance with the Declaration of Helsinki and approved by the Regional Committee of Human Ethics (Dnr 2011/285-31, 2012/216-31, 2013/111-31 and 2013/506-32). All subjects gave their written informed consent.

2.2 | Endoscopic and Histologic Grading of Inflammation

The extent of the inflammation was noted as the distance in centimeters from the anus and graded according to Endoscopic Mayo score (0–3) [16]. Histological activity was graded according to the modified Riley score [17] (range 0–7) and the Robarts index [18] (range 0–33) and Nancy histology index (NHI) [19] (range 0–4) by an experienced pathologist (S.I.).

2.3 | Healthy Control Group

Individuals (10 women and 6 men, median age 30 years [range 22–61 years]) with no medical history of chronic gastrointestinal symptoms and disorders, allergies and no intake of anti-inflammatory medication were recruited as a control group.

2.4 | Collection of Biopsies

Patients with UC received anti-inflammatory treatment according to Table 1. Colorectal biopsies were collected from the inflamed and non-inflamed segment 5 cm distal to the demarcation line and from non-inflamed segment 10 cm proximal to this line. Both biopsy locations were noted as the distance in cm from the anal verge. At the first visit, biopsies were collected both from inflamed distal colon and the non-inflamed proximal colon during clinically active UC (Figure 1). A follow-up sigmoidoscopy was performed once patients reached clinical and endoscopic remission and biopsies were obtained from the same location as the initial visit as outlined in the study overview. Biopsies from the healthy control group were obtained

TABLE 1 | Characteristics of the 14 patients with ulcerative colitis (UC) included in the study.

Patient ID	Age (year)	Sex	Allergy	Smoking	Inflamed segment biopsy location	Non-inflamed segment biopsy location	Disease location	Anti-inflammatory medication	
								1st visit	2nd visit
1	28	M	Penicillin	No	Sigmoideum	Sigmoideum	Rectosigmoideum	5-ASA, AZA	5-ASA, IFX
2	36	F	No	No	Rectum	Sigmoideum	Rectum	5-ASA	5-ASA
3	21	M	No	No	Rectum	Sigmoideum	Rectum	5-ASA	5-ASA
4	71	F	No	No	Rectum	Sigmoideum	Rectum	5-ASA	5-ASA
5	61	F	Pollen and fur	No	Sigmoideum	Sigmoideum	Rectosigmoideum	5-ASA	5-ASA
6	61	M	No	No	Sigmoideum	Sigmoideum	Rectosigmoideum	5-ASA, AZA	5-ASA
7	48	F	No	No	Rectum	Sigmoideum	Rectum	Steroids	5-ASA
8	20	F	No	No	Rectum	Sigmoideum	Rectum	None	5-ASA
9	34	M	No	Yes	Sigmoideum	Sigmoideum	Rectosigmoideum	5-ASA, AZA	AZA
10	21	M	Pollen	No	Sigmoideum	Sigmoideum	Rectosigmoideum	AZA	5-ASA, AZA
11	35	M	Pollen	No	Sigmoideum	Sigmoideum	Rectosigmoideum	5-ASA	5-ASA, steroids
12	41	M	No	No	Sigmoideum	Sigmoideum	Rectosigmoideum	5-ASA	5-ASA
13	72	F	No	No	Sigmoideum	Sigmoideum	Rectosigmoideum	None	5-ASA, AZA
14	64	M	No	No	Sigmoideum	Sigmoideum	Rectosigmoideum	5-ASA	5-ASA

Note: Biopsies were collected from 14 patients with clinically active UC (1st visit). Patients were given anti-inflammatory medication and returned for follow-up biopsies when in clinical and endoscopic remission (2nd visit). Biopsies were taken in October–December that is outside pollen season in Sweden.
Abbreviations: 5-ASA, 5-aminosalicylic acid; AZA, azathioprine; F, female; IFX, infliximab; M, male. Biopsies were taken in October–December that is outside pollen season in Sweden.

from the sigmoid colon during sigmoidoscopy. All biopsies were collected with forceps without a central lance and directly put in ice-cold oxygenated Krebs buffer [20].

2.5 | Immunofluorescence

Colorectal biopsies from all study groups were used for immunofluorescence studies of EGC markers as previously described [10]. Briefly, after fixation in 4% paraformaldehyde, biopsies were embedded in paraffin, sectioned (5 μm), and incubated at 60°C for 3 h. Standard deparaffinization and rehydration were followed by antigen retrieval in citrate buffer (10 mM, pH 6, with 0.5% Tween 20) through boiling and permeabilization in PBS-0.1% Triton 100X for 10 min. Sections were blocked with 1% BSA in PBS-0.5% Tween and 300 mM glycine for 30 min. Sections were stained with rabbit-anti-GFAP (1:500; Dako Cytomation, Denmark) or rabbit-anti-S100β (1:200; Abcam, Netherlands), followed by Alexa Fluor 546-conjugated secondary antibodies (1:1000; Invitrogen, Netherlands). Prolong Gold DAPI (Thermo Fisher, Sweden) was used for mounting. Secondary antibody specificity was confirmed by omitting primary antibodies. For quantification of glial cell bodies expressing GFAP (EGC^{GFAP+}) or S100β ($EGC^{S100\beta+}$), five 63× magnification images per sample were captured, using the same imaging settings, with a Leica DMi8 microscope (Leica Microsystems CMS, Wetzlar, Germany) equipped with Hamamatsu ORCA Flash 4 (SCMOS) camera (Hamamatsu, Hamamatsu City, Japan) and Leica software (Leica Microsystems CMS, Wetzlar, Germany). Manual counting was performed in a blinded manner using Fiji/ImageJ software [21] with results expressed as mean number of cells per mm^2.

2.6 | Protein Analysis and Protein Selection

For protein extraction, 196 μL of radioimmunoprecipitation assay (RIPA) buffer (Sigma, St. Louis, MO, USA) was combined with 4 μL of protease inhibitor (SigmaFast 50X) in an Eppendorf

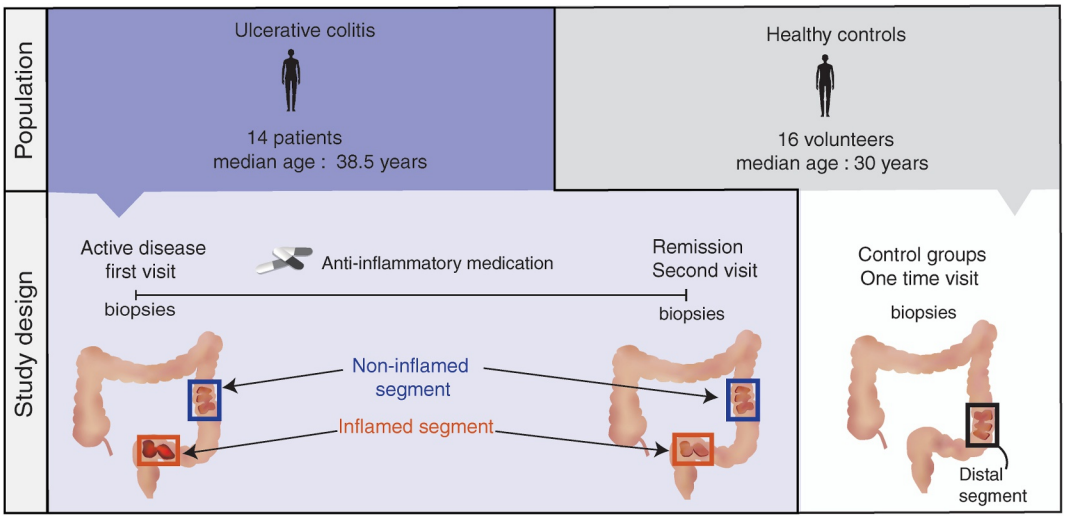

FIGURE 1 | Study design and biopsy sampling from 14 patients with ulcerative colitis (UC) and 16 healthy controls (HC). Patients with UC were recruited during a clinical flare up of the disease (active disease). Colorectal biopsies from UC were collected by sigmoidoscopy from the inflamed and non-inflamed segment during clinically active disease and in clinically and endoscopic remission after following anti-inflammatory medication. Biopsies from HC were collected by sigmoidoscopy from the distal colon only for a one-time visit.

tube. Biopsy samples were then added after carefully removing any residual Allprotect from the tissue. The mixture was sonicated on ice using 10 times 1-s pulses at 15% amplitude (Chemical Instrument AB, Lidingö, Sweden) to lyse cells and homogenize the sample. The homogenate was subsequently centrifuged at 16,000 *g* for 10 min at 4°C. The resulting supernatant was transferred to a cryotube and stored at −80°C.

Biopsies were analyzed by proximity extension assay using the Proseek Multiplex Inflammation I and Oncology II Probe kit (Olink Proteomics, Uppsala, Sweden), which includes 162 inflammation and oncology related proteins (see Table S1). Data normalization and standardization were performed using the Olink Wizard for GenEx (Multid Analysis, Sweden). In these steps, the Ct values of the qPCR were transformed into the arbitrary unit, normalized protein expression (NPX), which represents the relative protein levels on log2 scale [22]. In addition, total protein concentration of lysed material was determined using the Bio-Rad DC protein assay kit (Bio-Rad, Sweden) and the Modulus Microplate reader (Turner BioSystems, USA). A linear model was applied to adjust for differences because of varying total protein concentrations between lysates. The model was fitted for each protein i, using the measured total protein concentration c of each sample j with the intercept μ, coefficient β, and error ε.

$$\mathrm{NPX}_{i,j} = \mu_i + \beta_i \cdot \log 2(c_j) + \varepsilon_{i,j}.$$

We used the following formula to calculate the adjusted normalized protein expression (NPX) value of each protein i and sample j:

$$\mathrm{NPXadj}_{i,j} = \mathrm{NPX}_{i,j} - (\mu_i + \beta_i \cdot \log 2(c_j)) + \mathrm{mean}(\mathrm{NPX}_{i,j}).$$

Only proteins with significant positive correlation between their NPX value and the total protein concentration were adjusted. Proteins exhibiting significant negative correlation were excluded from the analyses due to concerns about data reliability issues, such as measurements exceeding the upper limit of detection. Data analyses were performed using R[17], version 4.05 and the packages ggplot2 [23], tidyverse [24], and ggrepel [25]. When no significant correlation was observed, the original values were kept. Relevant packages listed below were used for analysis. We further highlight a subset of proteins that were associated with EGC through a literature search using PubMed, including the ones having ≥ 2 hits when searching the term: "Enteric + glial + cells and gene symbol," where the gene symbol was provided in the Olink manifest (see R code, Supporting Information S1). Proteins associated with EGC were further analyzed in inflamed segments from patients with clinically active UC, those in remission and HC.

2.7 | In Vitro Experiments

The enteroglial rat cell line (ATCC, CRL-2690) was cultured according to standard operating procedures until sub-confluent in six well-plates (1×10^6 cells/mL). Cells were stimulated with Dulbecco's modified Eagle's medium (DMEM) (Invitrogen, Sweden) containing interleukins (IL)-4 or IL-6 at a concentration of 1, 10 or 100 ng/mL for 6 and 24 h. As controls, cells were added DMEM only. At the end of the timepoint, supernatants were collected, and cells were harvested using 0.25% trypsin [26]. The cell pellet and supernatant were stored for further analyses at −80°C.

2.8 | ELISA

Sandwich ELISA kits were used according to standard operating procedures to measure GFAP and S100β levels in supernatants from interleukin stimulated cells [26]. Briefly, samples were

added to plates pre-coated with primary antibodies, incubated at 37°C for 90 min, followed by secondary antibody addition and further 60-min incubation. Plates were processed according to manufacturer's instructions (Nordic Biosite, Sweden), and absorbance read at 450 nm using a VersaMax Microplate reader with SoftMax Pro 5 (Molecular Devices).

2.9 | Western Blot

Protein was extracted from frozen EGC and used for western blotting, as previously described [10]. Briefly, equal amounts of protein (10 μg per sample, assessed by DC protein assay [Biorad, USA]) were separated on a 4%–20% tris-glycine gel (Thermo Fisher, Sweden), transferred onto a nitrocellulose membrane, and blocked with 5% non-fat dry milk (Bio-Rad, USA). Membranes were incubated overnight at 4°C with specific primary antibodies (anti-GFAP, 1:1000, Dako Cytomation, Denmark; anti-S100β, Abcam, Netherlands; anti-β-actin, 1:10,000 [Cell Signaling, BioNordika, Sweden]). After washing, membranes were incubated with fluorescently labeled secondary antibodies (Alexa Fluor 790 anti-rabbit and Alexa Fluor 680 anti-mouse, 1:20,000 [Thermo Fisher, USA]). Fluorescent bands were detected using the Odyssey CLx system and quantified with Image Studio software (LI-COR Biosciences). The levels of GFAP, and β-actin loading control were corrected to their brightest signal within each membrane, and GFAP protein was then normalized to β-actin corrected values. Values are given as GFAP/β-actin standardized to control wells.

2.10 | Statistical Analysis

Data were analyzed using GraphPad Prism 10.0.2 (GraphPad Software Inc). Data normality was assessed using the Shapiro–Wilk test. Depending on normality, group comparisons were performed using ANOVA or Kruskal–Wallis, and comparisons between active UC and remission were analyzed using Student's *t*-test or Wilcoxon test. Significance was set as $p < 0.05$ with results expressed as mean ± SEM or median and interquartile range (IQR). For protein data, the analysis was performed using R[17], version 4.05, and relevant packages as listed in the method.

3 | Results

3.1 | Evaluation of Disease Activity and Histological Grading

At the first visit, during clinically active UC, all patients showed active disease with a median Full Mayo score of 7.5 (range 4–8) and Endoscopic Mayo score of 2 (range 1–2). At follow-up, all were in clinical (Full Mayo score ≤ 2) and endoscopic remission (Endoscopic Mayo score ≤ 1) (Table 2). Biopsies from non-inflamed segments had minimal histologic inflammation at both visits (median modified Riley score 0, Robarts 1 or 0, NHI 0). Inflamed areas during active disease showed higher inflammation (Riley median 4, Robarts 10; NHI 3 $p < 0.001$) compared to non-inflamed and remission samples. At follow-up,

TABLE 2 | Mayo score and histological grading of biopsies from the 14 patients with ulcerative colitis (UC) included in the study.

	Full Mayo score		Endoscopic Mayo score		Mod Riley score inflamed area		Mod Riley score non-inflamed area		Robarts score inflamed area		Robarts score non-inflamed area		Nancy score inflamed area		Nancy score non-inflamed area	
Patient ID	1st visit	2nd visit	1st visit	2nd visit	1st visit	2nd visit	1st visit	2nd visit	1st visit	2nd visit	1st visit	2nd visit	1st visit	2nd visit	1st visit	2nd visit
1	8	0	2	0	—	0	—	0	—	1	—	1	—	0	—	0
2	8	2	2	1	4	0	0	0	13	9	1	1	2	0	0	0
3	8	0	1	0	4	0	0	0	10	1	1	0	3	0	0	0
4	4	0	1	0	5	4	0	0	21	4	1	0	3	2	0	0
5	5	0	2	0	5	0	0	0	15	1	0	0	3	0	0	0
6	8	0	2	0	—	0	—	0	—	1	—	1	—	0	—	0
7	8	0	2	0	1	0	0	0	10	1	1	1	2	0	0	0
8	5	0	2	0	0	0	0	0	2	0	1	0	0	0	0	0
9	5	0	2	0	7	4	0	0	19	10	0	0	4	2	0	0
10	6	0	2	0	4	0	0	0	16	1	1	1	2	0	0	0
11	8	0	2	0	4	4	0	0	9	6	1	0	3	2	0	0
12	8	0	2	0	5	0	0	0	10	1	1	1	3	0	0	0
13	7	0	2	0	4	0	0	0	8	1	0	0	2	0	0	0
14	7	0	2	0	5	0	0	0	15	0	0	0	3	0	0	0

Note: The extension of the inflammation was noted as distance in cm from the anus and graded according to endoscopic Mayo score. Histological grade of inflammation was graded according to the modified Riley score, Robarts index and Nancy score. Evaluation was done in biopsies collected from 14 patients with clinically active UC (1st visit) and at follow-up when in clinical and endoscopic remission (2nd visit). Missing data is indicated with —.

Robarts scores remained slightly higher in previously inflamed versus non-inflamed segments ($p < 0.05$), while Riley scores and NHI did not differ (Table 2).

3.2 | EGC^{GFAP+} and $EGC^{S100\beta+}$ in Active Disease and Remission Compared to HC

The numbers of EGC^{GFAP+} were increased in the inflamed segment of the colon during clinically active UC compared to clinically and endoscopic remission ($p < 0.001$) (Figure 2A,B). Both EGC^{GFAP+} and $EGC^{S100\beta+}$ were higher in the inflamed segment of the colon during active UC compared to non-inflamed segment (EGC^{GFAP+} $p < 0.05$, $EGC^{S100\beta+}$ $p < 0.0001$) in active disease and remission ($p < 0.001$) (Figures 2A,B and 3A,B). Of note, levels of EGC^{GFAP+} after reaching remissions were reduced compared to the non-inflamed segments during active UC ($p < 0.05$) (Figure 2A). A reduction in inflamed segments for both markers was observed in 13 out of 14 patients reaching remission ($p < 0.001$) (Figures 2C and 3C). EGC^{GFAP+} decreased in non-inflamed segments, when patients reached remission, $p < 0.001$ (Figure 2C), whereas levels of $EGC^{S100\beta+}$ remained unaltered (Figure 3C). When compared to HC, EGC^{GFAP+} and $ECG^{S100\beta+}$ numbers were elevated in inflamed segments of patients with active UC ($p < 0.0001$) and in those in remission (EGC^{GFAP+}, $p < 0.05$, $EGC^{S100\beta+}$ $p < 0.01$) (Figures 2B and 3B). Only EGC^{GFAP+} was increased in non-inflamed segments of patients with active UC ($p < 0.001$) and remission ($p < 0.05$) when compared to HC (Figure 2B). No difference was observed in levels of $EGC^{S100\beta+}$ in the non-inflamed segments of UC as compared to HC (Figure 3B).

3.3 | EGC-Associated Protein Levels in Clinical Active Disease and in Remission

Of the 162 proteins analyzed, 10 were identified as EGC-associated based on ≥ 2 PubMed hits of relevant scientific publications. These proteins fell into four categories: pro-inflammatory cytokines (TNF, IL-6, IFN-γ, IL-18), neurotrophic/neuroprotective factors (NT-3, RET, and GDNF), chemokines (CXCL10 and IL-8), and anti-inflammatory cytokine (IL-4) (Figure 4A). We next tested the differences in the relative protein levels of these 10 proteins between inflamed and non-inflamed segments during active disease, remission and HC. An upregulation was observed in seven out of 10 EGC-associated proteins in inflamed versus non-inflamed segments during active disease (Figure 4B). When comparing inflamed segments in active disease to remission, eight out of 10 proteins were found to be elevated (Figure 4C). When

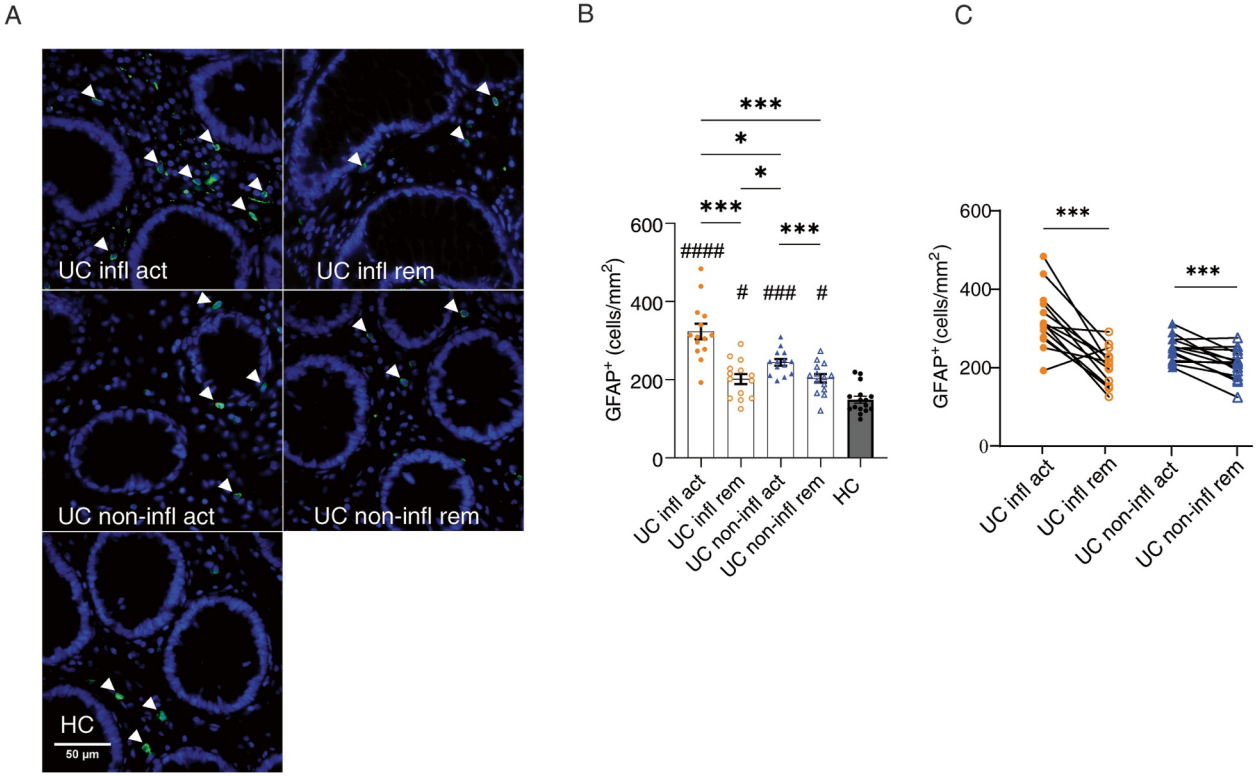

FIGURE 2 | Colorectal biopsies from 14 patients with ulcerative colitis (UC) and 16 healthy controls (HC) were sectioned and stained for glial fibrillary acidic protein (GFAP) and manually quantified. (A) Representative images of EGC^{GFAP+} (green, arrowheads) staining in patients with UC (patients during clinically active disease and clinical remission both from the inflamed and non-inflamed segment), as well as from HC. Scale bar = 50 µm. (B) Number of EGC^{GFAP+}/mm^2 in patients with UC during clinically active and remission in the inflamed (orange) and non-inflamed segment (blue) compared to HC (gray). (C) Levels of EGC^{GFAP+} decreased in 13 out of 14 patients in the inflamed segment and 11 out of 14 in the non-inflamed segment between clinically active UC and remission. Data are expressed as mean ± SEM, one-way ANOVA, Student's *t*-test $^{\#}p < 0.05$, $^{\#\#\#}p < 0.001$, $^{\#\#\#\#}p < 0.001$ when compared to HC. $^{*}p < 0.05$, $^{***}p < 0.001$. Act, active; infl, inflamed; rem, remission.

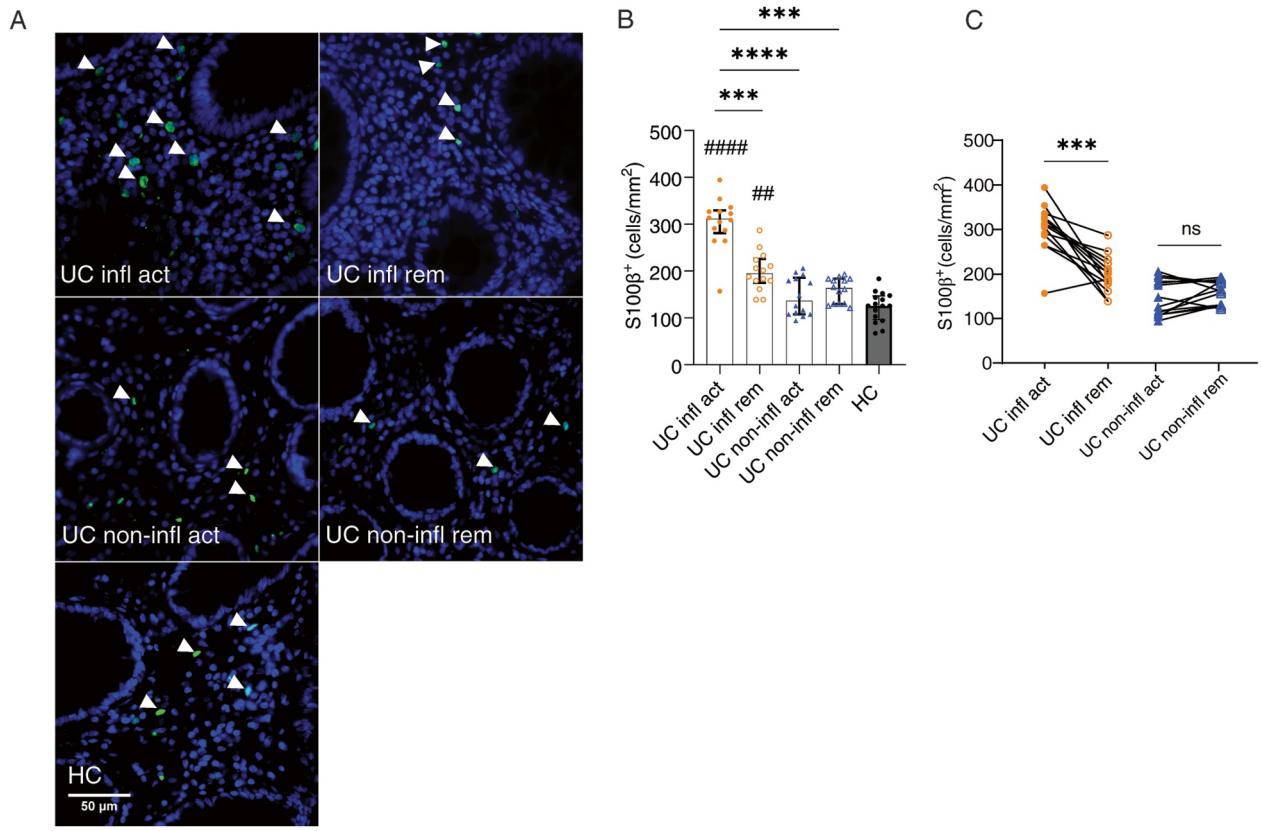

FIGURE 3 | Colorectal biopsies from 14 patients with ulcerative colitis (UC) and 16 healthy controls (HC) were sectioned and stained for S100 calcium-binding protein β (S100β) and manually quantified. (A) Representative images of $EGC^{S100\beta+}$ (green, arrowheads) staining in patients with UC (patients during clinically active disease and clinical remission both from the inflamed and non-inflamed segment), as well as from HC. Scale bar = 50 µm. (B) Number of $EGC^{S100\beta+}/mm^2$ in patients with UC during clinically active and remission in the inflamed (orange) and non-inflamed segment (blue) compared to HC (gray). (C) Levels of $EGC^{S100\beta+}$ decreased in 13 out of 14 patients in the inflamed segment while no difference in the non-inflamed segment when comparing clinically active disease and remission. Data are expressed as median (IQR), Kruskal–Wallis test, Wilcoxon test, $^{\#\#}p < 0.01$, $^{\#\#\#\#}p < 0.001$ when compared to HC $^{***}p < 0.001$, $^{****}p < 0.0001$. Act, active; infl, inflamed; ns, non-significant; rem, remission.

compared to HC, nine out of 10 proteins were upregulated during active UC in the inflamed segments (Figure 4D). An upregulation of IL-8 was found when comparing non inflamed segment during active UC to HC (Figure 4E). All differences in protein levels observed in the inflamed segment at active disease returned to levels comparable to the non-inflamed segment in remission or to HC (Figure S1A,B). There was no difference in the protein levels of the non-inflamed segment at active disease versus remission (Figure S1C). However, when comparing non-inflamed segments in both active disease and remission (Figure S1D) to HC, a significant downregulation of IL-8 was observed.

Several proteins were highly upregulated in the inflamed segment during active UC, and despite not being directly linked to EGC, they all have known glial and neuronal functions in the central nervous system (CNS). The most elevated proteins included IL17-A, TNFRSF6B, WISP1, oncostatin M (OSM) and multiple CXCL protein family (CXCL9, 5, and 11), particularly when comparing inflamed to non-inflamed segments (Figure S2A). Some of these (IL-17A, TNFRSF6B, WISP1, CXCL9, and OSM) were also upregulated compared to HC. Additionally, ADAM 8, PDL1, and CXCL11 showed notable increases (Figure S2B).

3.4 | Modulation of GFAP Expression by Interleukin Stimulation

Stimulation with IL-6 (10 ng/mL) induced a threefold increase in GFAP expression of the EGC line CRL-2690 at 6 h and a fourfold increase at 24 h (Figure 5A,C). A similar expression pattern was observed after stimulation with IL-6 at 100 ng/mL and reaching a sixfold peak at 24 h. No upregulation of GFAP expression was observed in response to 1 ng/mL IL-6 at 6 or 24 h (Figure 5A,C). In contrast, IL-4 at 1 ng/mL reduced GFAP expression after both 6 and 24 h, whereas stimulation with 10 and 100 ng/mL IL-4 had no effect (Figure 5B). The quantification of S100β by western blotting was detectable but the signal was not enough to provide accurate results (data not shown). Quantification of GFAP and S100β in supernatants from stimulated cells using ELISA were under the detection level, regardless of interleukin, concentration, and time duration of exposure (data not shown).

4 | Discussion

The present study provides novel insights into the role of EGC in UC, particularly focusing on the abundance and expression of

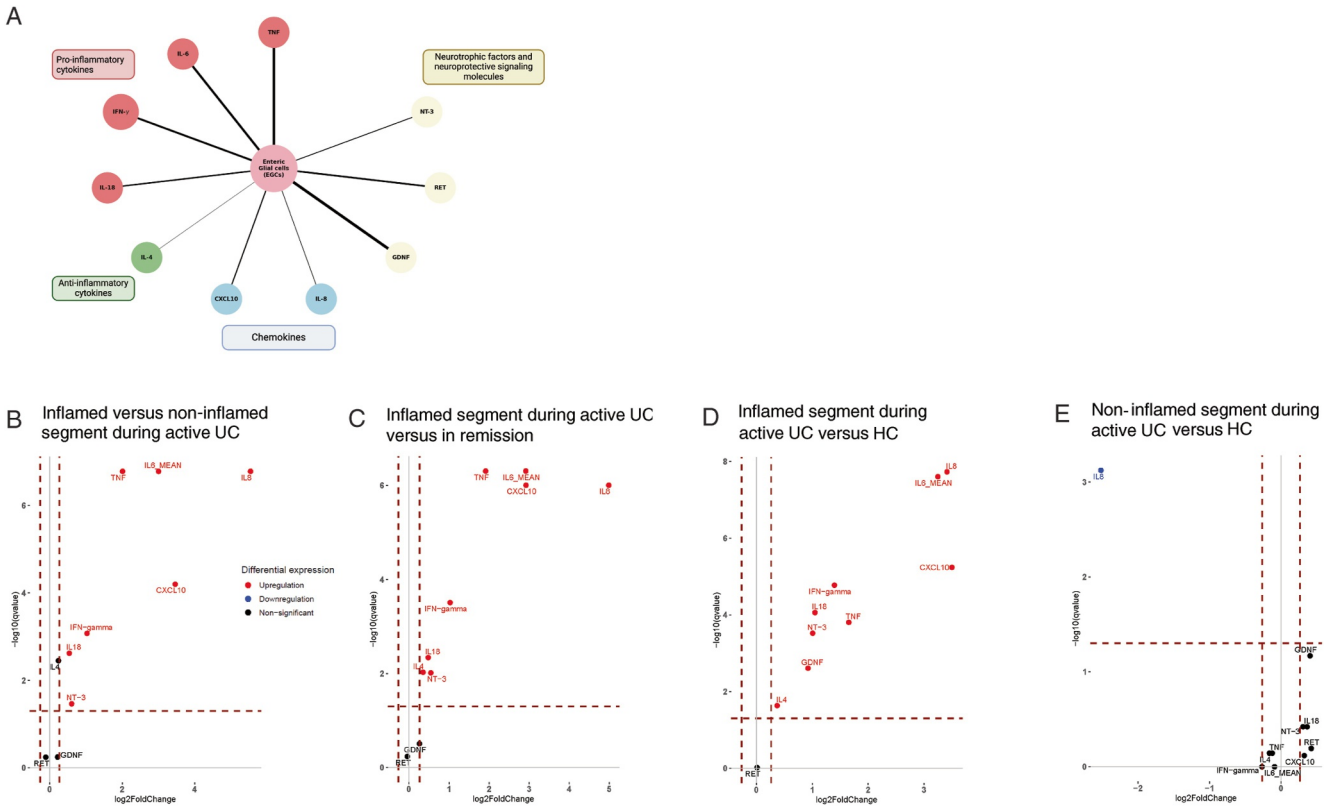

FIGURE 4 | Differentially expressed enteric glial cell (EGC)-associated proteins in ulcerative colitis (UC) state in inflamed and non-inflamed segments or as compared to healthy controls (HC). Of the 162 proteins analyzed, 10 were identified as associated with EGC based on a minimum of two relevant PubMed references. (A) Overview of the proteins falling into four categories: pro-inflammatory cytokines in red (TNF, IL-6, IFN-γ, IL-18), neurotrophic and neuroprotective factors in yellow (NT-3, RET, glial cell line derived neurotrophic factor [GDNF]), chemokines in blue (CXCL10, IL-8), and anti-inflammatory cytokines in green (IL-4). The thickness of the lines represents the number of hits of relevant articles in PubMed. (B) Inflamed versus non-inflamed segment during active UC. (C) Inflamed segment during active UC versus in remission. (D) Inflamed segment during active UC versus HC. (E) Non-inflamed segment during active UC versus HC. Upregulated and downregulated proteins are shown as red and blue respectively. Non-significant proteins are shown in black. log2 fold change is shown on the *x*-axis. The parallel dotted line represents the threshold set for $p < 0.05$, −log10 (adj. *p*. value) represents inverted adjusted *p*-value.

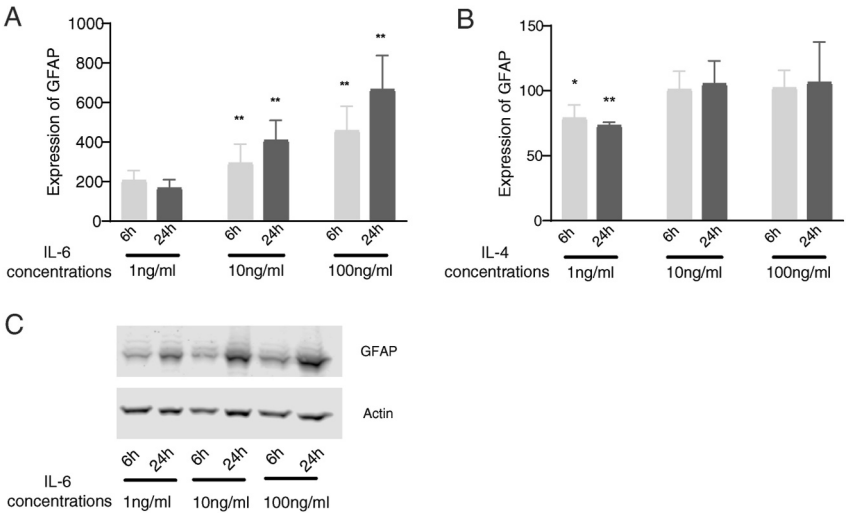

FIGURE 5 | Modulation of glial fibrillary acidic protein (GFAP) expression by interleukin stimulation. Sub-confluent enteric glial cells (EGC) were incubated with 1, 10 or 100 ng/mL of IL-6 (A) or IL-4 (B) for 6 or 24 h. Representative western blot image for IL-6. (C) The expressions of GFAP in the cell pellets and the housekeeping protein β-actin were quantified by western blotting. GFAP expression was normalized to control wells for each time point. Controls were standardized and set at 100% and each sample is expressed in percentage. Data are expressed as median (IQR) of three independent experiments, Mann–Whitney test, $*p < 0.05$, $**p < 0.01$.

EGC^{GFAP+} and $EGC^{S100\beta+}$ within the same patients across active inflammation and remission. Notably, we could observe differences when comparing EGC^{GFAP+} and $EGC^{S100\beta+}$ levels for the non-inflamed segment. Because our quantification approach employed single-marker rather than double-label staining, we could not determine whether GFAP and S100β are co-expressed in the same cell or identify distinct EGC subpopulations. However, previous studies highlighted that GFAP and S100β are expressed differentially and do not consistently overlap [27]. Further studies incorporating co-localization techniques and/or immunostaining for additional markers such as PLP1 and Sox10 would be relevant.

In this study, the observed upregulation of EGC^{GFAP+} and $EGC^{S100\beta+}$ within the inflamed regions during active UC aligns with prior studies emphasizing the involvement of EGC in intestinal barrier dysfunction and promoting inflammation [12, 14] The abundance of EGC observed in our data suggest both a reactive response to inflammatory mediators and, a potential contribution to the propagation of mucosal inflammation which could lead to perpetuating inflammation in UC.

Previous studies using western blot [28], immunohistochemistry [11], and immunocytochemistry [12] have reported a GFAP overexpression in inflamed biopsies from UC patients group (mixing both active and non-active cases) compared with non-inflamed areas [11] or HC [12, 28]. Whereas most earlier studies focused on S100β in active UC, none investigated patients in remission or followed UC states. One study investigated the role of S100β using immunohistochemistry from the inflamed and non-inflamed segment without successful results [3]. A second study, using the same methodology showed a reduction in myenteric $EGC^{S100\beta+}$ when comparing the inflamed segment to HC [29]. Here, we demonstrated that the number of $EGC^{S100\beta+}$ is upregulated in patients with UC during active disease. This has not been observed before when using immunofluorescence and is consistent with our recent findings in ileum of patients with CD, where EGC were found to be associated with impaired barrier function and more abundant in both lamina propria and Peyer's patches areas compared to non-IBD [10]. Despite methodological differences, these results align with previous studies reporting increased S100β protein expression and release from samples of patients with active UC compared with HC [9, 30]. Taken together, these findings indicate that an increased level of EGC^{GFAP+} and $EGC^{S100\beta+}$ are associated with both UC and CD inflammation and may play a significant role in both ileal and colonic inflammation. We observed a significant reduction in the expression of EGC markers during remission, indicating the potential of anti-inflammatory treatment to reverse the number of EGC. Of note, these reductions were observed in the context of minimal histological inflammation, highlighting the sensitivity of EGC markers changes to subtle shifts during inflammatory activity. This supports the hypothesis that upregulation of EGC, and reactive EGC, is driven by the inflammatory environment and may not be an inherent characteristic of UC [13, 15].

The antigen-presenting potential of EGC, as demonstrated in the study by Brown et al., adds another layer of complexity to their role in UC. Emerging evidence suggests that EGC may play a crucial role in modulating adaptive immunity during intestinal inflammation [31]. Potentially, by regulating CD8+T cells via MHCI mediated antigen presentation in inflammatory conditions. Notably, CD8+T cells have been identified as key initiators of the inflammatory process and the development of gut lesions during CD [32]. This aligns with our present findings, where cytokine-driven modulation of EGC markers was evident, particularly through IL-6-mediated upregulation of GFAP. The interplay between EGC and immune cells, such as CD8+T cells, might contribute to the perpetuation of inflammation in UC [33]. In contrast, IL-4 caused a decrease in GFAP at 6 and 24 h which is in line with a previous study, where a slight decrease was observed in rat isolated EGC [34].

Notably, the reactive status of EGC is not only observed when comparing cell numbers. A protective role of EGC-secreted factors, seen by an increase of GDNF in the submucosal plexus of inflamed colonic biopsies, has been described in IBD [12]. Moreover, a rotavirus study highlights a contrasting role for neurotrophic factors, such as GDNF, which protects the intestinal barrier during viral infections by enhancing tight junction integrity and reducing epithelial permeability [35]. This protective role contrasts with their pro-inflammatory and barrier-compromising effects in UC, emphasizing the context dependent functionality of EGC. The persistent barrier dysfunction observed in the same cohort of patients with UC during remission compared to HC [36], could influence EGC reactivity and help explain why no upregulation of GDNF, or its precursor RET, is observed with proteomic analysis. In UC, it appears that the inflammatory cytokine milieu skews EGC to promote barrier dysfunction and contribute to inflammation, as opposed to the protective roles seen during viral challenges.

Even though the search for gene symbols is conservative and more associations might be found, the proteomic data in this study aims to highlight the dynamic nature of EGC involvement in inflammation. The upregulation of pro-inflammatory proteins during active disease and their reduction during remission parallels previous observations in irritable bowel syndrome, where EGC-derived mediators influenced permeability without a clear inflammatory profile [20]. The specificity of these changes to UC suggests that EGC are finely tuned to the inflammatory context of the disease. However, even though identified as EGC-associated, proteins are also more or less expressed by other cell types and known to be elevated during inflammation. As per example, to the best of our knowledge, no studies investigated the role of IL-8 with EGC, but IL-8 was highlighted for its role in UC, as it appeared to be the most frequently expressed cytokine across all Mayo endoscopic subscores categories, underscoring its potential as a sensitive marker of mucosal inflammation [37].

Several highly upregulated proteins in inflamed UC segments, beyond those directly related to EGC, have known glial and neuronal functions in the CNS. IL-17A has previously shown a pronounced increase in UC compared to HC [38], and in the CNS, IL-17A contributes to neuroinflammation via oligodendrocytes [39]. Similarly, OSM, also implicated in IBD pathogenesis [40] and CXCL9, have shown to be produced by microglia [41, 42]. Protective or regulatory proteins including ADAM8 (neuroprotection) [43] and PD-L1 expression, which microglia use to modulate T-cell effector function to limit

damage, were also upregulated [44]. Finally, WISP1 and TNFRSF6B, known for promoting microglial survival in Alzheimer's disease [45, 46] showed increased expression in inflamed UC segments, emphasizing the context-dependent role of glial cells. Further research on glial cell function is essential to determine whether their role in the CNS can be applied to EGC.

In summary, this study reinforces the duality of EGC functions in intestinal homeostasis and disease. The upregulation of EGC markers during UC highlights their role as amplifiers of inflammation and potential contributors to barrier dysfunction, by reacting to inflammatory signals, while their downregulation during remission suggests they could be harnessed in a clinical perspective. Nevertheless, this study has some limitations, including the relatively small sample size and single-center design. In addition, the reliance on marker-based identification of EGC subtypes may not fully capture the functional heterogeneity of these cells. Future research should explore the molecular pathways driving EGC activation and their interactions with immune cells, to uncover novel interventions that modulate glial activity and restore gut barrier integrity in UC.

Author Contributions

Julie Beaudeau: data curation, visualization, writing – review and editing, methodology, investigation, writing – original draft, formal analysis, validation. **Georgios Katinios:** writing – review and editing, data curation, investigation, validation, visualization. **Carl Mårten Lindqvist:** writing – review and editing, methodology, data curation, formal analysis, visualization, software, validation, investigation. **Susanna A. Walter:** writing – review and editing, supervision, data curation, investigation, resources. **Simone Ignatova:** writing – review and editing, data curation, validation. **Olga Bednarska:** writing – review and editing, data curation, investigation. **Andreas Münch:** writing – review and editing, investigation, data curation. **Johan D. Söderholm:** writing – review and editing, validation, supervision, resources. **Jonas Halfvarson:** writing – review and editing, data curation, investigation, validation, resources. **Benita Salomon:** writing – review and editing, data curation, investigation, software, validation. **Ida Schoultz:** writing – review and editing, methodology, writing – original draft, data curation, visualization. **Henrik Hjortswang:** conceptualization, writing – review and editing, data curation, investigation, resources. **Åsa V Keita:** conceptualization, funding acquisition, writing – review and editing, supervision, validation, methodology, project administration, resources.

Acknowledgments

We thank all patients and healthy volunteers for participating. We also thank Mr. Martin E. Winberg, Linköping University, for sectioning and assistance with in vitro and western blotting experiments. The Core Facility, Faculty of Medicine and Health Sciences, Linköping University, is acknowledged for support with epifluorescence microscopy. This work was supported by grants from "Stiftelsen Professor Nanna Swartz fond" (Å.V.K.); "Stiftelsen Apotekare Hedbergs Fond för Medicinsk Forskning" (Å.V.K.); Medical Faculty, Linköping University (Å.V.K.); "Ruth and Richard Julin Foundation" (Å.V.K.); "Region Östergötland (Grant RÖ-969343)" (Å.V.K.).

Disclosure

Part of the material was presented at the 20th ECCO Congress 2025 in Berlin, Germany (https://doi.org/10.1093/ecco-jcc/jjae190.0342). Previous work using the same patient material was presented at the 14th ECCO Congress 2019 in Copenhagen, Denmark (https://doi.org/10.1093/ecco-jcc/jjy222.215).

Conflicts of Interest

H.H. and J.H. have received consulting, advisory, speaker, or teaching fees from AbbVie, Eli Lilly, Ferring, Janssen, Pfizer, Takeda, and Tillotts Pharma. H.H. also received advisory or teaching fees from: Fresenius Kabi, Norgine, Pharmacosmos. J.H. has additionally received consulting and/or advisory board fees from Alfasigma, Aqilion, Bristol Myers Squibb, Celgene, Celltrion, Galapagos, Gilead, Hospira, Index Pharma, Johnson & Johnson, MEDA, Medivir, Medtronic, Merck, Merck Sharp & Dohme, Novartis, Prometheus Laboratories Inc., Sandoz, Shire, STADA, Thermo Fisher Scientific, Vifor Pharma, UCB; speaker's fees from: Alfasigma, Bristol Myers Squibb, Celgene, Galapagos, Gilead, Hospira, Johnson & Johnson, Merck Sharp & Dohme, Novartis, Shire, Thermo Fisher Scientific; research grant support from: Janssen, Merck Sharp & Dohme, Takeda. The rest of the authors do not have any conflicts of interest to declare.

Data Availability Statement

Because of privacy considerations involving the patients and healthy control participants, the underlying data for this article cannot be made publicly available. However, the data may be accessed upon reasonable request by contacting the corresponding author.

References

1. C. Le Berre, S. Honap, and L. Peyrin-Biroulet, "Ulcerative Colitis," *Lancet* 402, no. 10401 (2023): 571–584, https://doi.org/10.1016/S0140-6736(23)00966-2.

2. J. D. Feuerstein, A. C. Moss, and F. A. Farraye, "Ulcerative Colitis," *Mayo Clinic Proceedings* 94, no. 7 (2019): 1357–1373, https://doi.org/10.1016/j.mayocp.2019.01.018.

3. V. Villanacci, G. Bassotti, R. Nascimbeni, et al., "Enteric Nervous System Abnormalities in Inflammatory Bowel Diseases," *Neurogastroenterology & Motility* 20, no. 9 (2008): 1009–1016, https://doi.org/10.1111/j.1365-2982.2008.01146.x.

4. J. Gonzales and B. D. Gulbransen, "The Physiology of Enteric Glia," *Annual Review of Physiology* 87, no. 1 (2024): 353–380, https://doi.org/10.1146/annurev-physiol-022724-105016.

5. L. Van Landeghem, J. Chevalier, M. M. Mahe, et al., "Enteric Glia Promote Intestinal Mucosal Healing via Activation of Focal Adhesion Kinase and Release of proEGF," *American Journal of Physiology - Gastrointestinal and Liver Physiology* 300, no. 6 (2011): G976–G987, https://doi.org/10.1152/ajpgi.00427.2010.

6. C. Le Berre, P. Naveilhan, and M. Rolli-Derkinderen, "Enteric Glia at Center Stage of Inflammatory Bowel Disease," *Neuroscience Letters* 809 (2023): 137315, https://doi.org/10.1016/j.neulet.2023.137315.

7. S. Coquenlorge, L. Van Landeghem, J. Jaulin, et al., "The Arachidonic Acid Metabolite 11β-ProstaglandinF2α Controls Intestinal Epithelial Healing: Deficiency in Patients With Crohn's Disease," *Scientific Reports* 6, no. 1 (2016): 25203, https://doi.org/10.1038/srep25203.

8. C. Pochard, S. Coquenlorge, J. Jaulin, et al., "Defects in 15-HETE Production and Control of Epithelial Permeability by Human Enteric Glial Cells From Patients With Crohn's Disease," *Gastroenterology* 150, no. 1 (2016): 168–180, https://doi.org/10.1053/j.gastro.2015.09.038.

9. G. Bassotti, V. Villanacci, R. Nascimbeni, et al., "Enteric Neuroglial Apoptosis in Inflammatory Bowel Diseases," *Journal of Crohn's and Colitis* 3, no. 4 (2009): 264–270, https://doi.org/10.1016/j.crohns.2009.06.004.

10. O. Biskou, F. Meira de-Faria, S. M. Walter, et al., "Increased Numbers of Enteric Glial Cells in the Peyer's Patches and Enhanced Intestinal

Permeability by Glial Cell Mediators in Patients With Ileal Crohn's Disease," *Cells* 11 (2022): 335, https://doi.org/10.3390/cells11030335.

11. A. Cornet, T. C. Savidge, J. Cabarrocas, et al., "Enterocolitis Induced by Autoimmune Targeting of Enteric Glial Cells: A Possible Mechanism in Crohn's Disease?," *Proceedings of the National Academy of Sciences* 98, no. 23 (2001): 13306–13311, https://doi.org/10.1073/pnas.231474098.

12. G. B. Von Boyen, N. Schulte, C. Pflüger, U. Spaniol, C. Hartmann, and M. Steinkamp, "Distribution of Enteric Glia and GDNF During Gut Inflammation," *BMC Gastroenterology* 11, no. 1 (2011): 3, https://doi.org/10.1186/1471-230x-11-3.

13. C. Cirillo, G. Sarnelli, G. Esposito, et al., "Increased Mucosal Nitric Oxide Production in Ulcerative Colitis Is Mediated in Part by the Enteroglial-Derived S100B Protein," *Neurogastroenterology & Motility* 21, no. 11 (2009): 1209, https://doi.org/10.1111/j.1365-2982.2009.01346.x.

14. D. Grundmann, E. Loris, S. Maas-Omlor, et al., "Enteric Glia: S100, GFAP, and Beyond," *Anatomical Record* 302, no. 8 (2019): 1333–1344, https://doi.org/10.1002/ar.24128.

15. F. Ochoa-Cortes, F. Turco, A. Linan-Rico, et al., "Enteric Glial Cells: A New Frontier in Neurogastroenterology and Clinical Target for Inflammatory Bowel Diseases," *Inflammatory Bowel Diseases* 22, no. 2 (2016): 433–449, https://doi.org/10.1097/MIB.0000000000000667.

16. K. W. Schroeder, W. J. Tremaine, and D. M. Ilstrup, "Coated Oral 5-Aminosalicylic Acid Therapy for Mildly to Moderately Active Ulcerative Colitis. A Randomized Study," *New England Journal of Medicine* 317, no. 26 (1987): 1625–1629, https://doi.org/10.1056/NEJM198712243172603.

17. B. G. Feagan, G. R. Greenberg, G. Wild, et al., "Treatment of Ulcerative Colitis With a Humanized Antibody to the $\alpha_4\beta_7$ Integrin," *New England Journal of Medicine* 352, no. 24 (2005): 2499–2507, https://doi.org/10.1056/nejmoa042982.

18. M. H. Mosli, B. G. Feagan, G. Zou, et al., "Development and Validation of a Histological Index for UC," *Gut* 66, no. 1 (2017): 50–58, https://doi.org/10.1136/gutjnl-2015-310393.

19. A. Marchal-Bressenot, J. Salleron, C. Boulagnon-Rombi, et al., "Development and Validation of the Nancy Histological Index for UC," *Gut* 66, no. 1 (2017): 43–49, https://doi.org/10.1136/gutjnl-2015-310187.

20. O. Biskou, S. Walter, H. Israelsen, M. E. Winberg, O. Bednarska, and ÅV. Keita, "ReFerm((R)): A Postbiotic Fermented Oat Gruel Composition Is Reducing Mast Cell Degranulation in the Colon of Patients With Irritable Bowel Syndrome," *Frontiers of Medicine* 11 (2024): 1408623, https://doi.org/10.3389/fmed.2024.1408623.

21. J. Schindelin, I. Arganda-Carreras, E. Frise, et al., "Fiji: An Open-Source Platform for Biological-Image Analysis," *Nature Methods* 9, no. 7 (2012): 676–682, https://doi.org/10.1038/nmeth.2019.

22. Olink Proteomics. White Paper, Data Normalization and Standardization, 1096, v2.1, 2022-04-08, accessed November 1, 2024, https://olink.com/knowledge/documents/.

23. W. Hadley, *ggplot2: Elegant Graphics for Data Analysis* (Springer-Verlag, 2016).

24. H. Wickham, M. Averick, J. Bryan, et al., "Welcome to the Tidyverse," *Journal of Open Source Software* 4, no. 43 (2019): 1686, https://doi.org/10.21105/joss.01686.

25. K. Slowikowski, "ggrepel: Automatically Position Non-Overlapping Text Labels With 'ggplot2'," R Package Version 0.9.3 (2023).

26. F. Meira de-Faria, M. Casado-Bedmar, C. Marten Lindqvist, et al., "Altered Interaction Between Enteric Glial Cells and Mast Cells in the Colon of Women With Irritable Bowel Syndrome," *Neurogastroenterology & Motility* 33 (2021): e14130, https://doi.org/10.1111/nmo.14130.

27. W. Boesmans, R. Lasrado, P. Vanden Berghe, and V. Pachnis, "Heterogeneity and Phenotypic Plasticity of Glial Cells in the Mammalian Enteric Nervous System," *Glia* 63, no. 2 (2015): 229–241, https://doi.org/10.1002/glia.22746.

28. G. Esposito, E. Capoccia, F. Turco, et al., "Palmitoylethanolamide Improves Colon Inflammation Through an Enteric Glia/Toll Like Receptor 4-Dependent PPAR-Alpha Activation," *Gut* 63, no. 8 (2014): 1300–1312, https://doi.org/10.1136/gutjnl-2013-305005.

29. N. Bernardini, C. Segnani, C. Ippolito, et al., "Immunohistochemical Analysis of Myenteric Ganglia and Interstitial Cells of Cajal in Ulcerative Colitis," *Journal of Cellular and Molecular Medicine* 16, no. 2 (2012): 318–327, https://doi.org/10.1111/j.1582-4934.2011.01298.x.

30. C. Cirillo, G. Sarnelli, G. Esposito, F. Turco, L. Steardo, and R. Cuomo, "S100B Protein in the Gut: The Evidence for Enteroglial-Sustained Intestinal Inflammation," *World Journal of Gastroenterology* 17, no. 10 (2011): 1261–1266, https://doi.org/10.3748/wjg.v17.i10.1261.

31. R. M. Brown, H. H. Le, I. W. Babcock, T. H. Harris, and A. Gaultier, "Functional Analysis of Antigen Presentation by Enteric Glial Cells During Intestinal Inflammation," *Glia* 73, no. 2 (2024): 291–308, https://doi.org/10.1002/glia.24632.

32. G. Boschetti, S. Nancey, D. Moussata, et al., "Enrichment of Circulating and Mucosal Cytotoxic CD8+ T Cells is Associated With Postoperative Endoscopic Recurrence in Patients With Crohn's Disease," *Journal of Crohn's and Colitis* 10, no. 3 (2016): 338–345, https://doi.org/10.1093/ecco-jcc/jjv211.

33. R. Casalegno Garduno and J. Dabritz, "New Insights on CD8(+) T Cells in Inflammatory Bowel Disease and Therapeutic Approaches," *Frontiers in Immunology* 12 (2021): 738762, https://doi.org/10.3389/fimmu.2021.738762.

34. G. B. T. Von Boyen, M. Steinkamp, M. Reinshagen, K. H. Schäfer, G. Adler, and J. Kirsch, "Proinflammatory Cytokines Increase Glial Fibrillary Acidic Protein Expression in Enteric Glia," *Gut* 53, no. 2 (2004): 222–228, https://doi.org/10.1136/gut.2003.012625.

35. M. Hagbom, F. M. De Faria, M. E. Winberg, et al., "Neurotrophic Factors Protect the Intestinal Barrier From Rotavirus Insult in Mice," *mBio* 11, no. 1 (2020): 20200121, https://doi.org/10.1128/mBio.02834-19.

36. G. Katinios, M. Casado-Bedmar, S. A. Walter, et al., "Increased Colonic Epithelial Permeability and Mucosal Eosinophilia in Ulcerative Colitis in Remission Compared With Irritable Bowel Syndrome and Health," *Inflammatory Bowel Diseases* 26, no. 7 (2020): 974–984, https://doi.org/10.1093/ibd/izz328.

37. K. Uchiyama, T. Takagi, K. Mizushima, et al., "Mucosal Cytokine Expression Associated With Deep Endoscopic Mucosal Healing in Ulcerative Colitis," *Journal of Crohn's and Colitis* 19, no. 3 (2025): jjae158, https://doi.org/10.1093/ecco-jcc/jjae158.

38. M. Matijasic, A. Baresic, H. Cipcic Paljetak, et al., "Serum Proteins and Faecal Microbiota as Potential Biomarkers in Newly Diagnosed, Treatment-Naive Inflammatory Bowel Disease and Irritable Bowel Syndrome Patients," *Journal of Molecular Medicine (Berlin)* (2025): 20250607, https://doi.org/10.1007/s00109-025-02558-5.

39. F. Kolbinger, C. Huppertz, A. Mir, and F. Padova, "IL-17A and Multiple Sclerosis: Signaling Pathways, Producing Cells and Target Cells in the Central Nervous System," *Current Drug Targets* 17, no. 16 (2016): 1882–1893, https://doi.org/10.2174/1389450117666160307144027.

40. S. Verstockt, B. Verstockt, and S. Vermeire, "Oncostatin M as a New Diagnostic, Prognostic and Therapeutic Target in Inflammatory Bowel Disease (IBD)," *Expert Opinion on Therapeutic Targets* 23, no. 11(2019): 943–954, https://doi.org/10.1080/14728222.2019.1677608.

41. J. R. Lokensgard, M. B. Mutnal, S. Prasad, W. Sheng, and S. Hu, "Glial Cell Activation, Recruitment, and Survival of B-Lineage Cells Following MCMV Brain Infection," *Journal of Neuroinflammation* 13, no. 1 (2016): 114, https://doi.org/10.1186/s12974-016-0582-y.

42. C. Chipoy, M. Berreur, S. Couillaud, et al., "Downregulation of Osteoblast Markers and Induction of the Glial Fibrillary Acidic Protein

by Oncostatin M in Osteosarcoma Cells Require PKCdelta and STAT3," *Journal of Bone and Mineral Research* 19, no. 11(2004): 1850–1861, https://doi.org/10.1359/JBMR.040817.

43. H. E. Hsia, J. Tushaus, T. Brummer, Y. Zheng, S. D. Scilabra, and S. F. Lichtenthaler, "Functions of 'A Disintegrin and Metalloproteases (Adams)' in the Mammalian Nervous System," *Cellular and Molecular Life Sciences* 76, no. 16(2019): 3055–3081, https://doi.org/10.1007/s00018-019-03173-7.

44. P. Chauhan and J. R. Lokensgard, "Glial Cell Expression of PD-L1," *International Journal of Molecular Sciences* 20, no. 7 (2019): 1677, https://doi.org/10.3390/ijms20071677.

45. Y. C. Shang, Z. Z. Chong, S. Wang, and K. Maiese, "Wnt1 Inducible Signaling Pathway Protein 1 (WISP1) Targets PRAS40 to Govern Beta-Amyloid Apoptotic Injury of Microglia," *Current Neurovascular Research* 9, no. 4 (2012): 239–249, https://doi.org/10.2174/156720212803530618.

46. Y. L. Liu, W. T. Chen, Y. Y. Lin, P. H. Lu, S. L. Hsieh, and I. H. J. Cheng, "Amelioration of Amyloid-Beta-Induced Deficits by DcR3 in an Alzheimer's Disease Model," *Molecular Neurodegeneration* 12, no. 1 (2017): 30, https://doi.org/10.1186/s13024-017-0173-0.

Supporting Information

Additional supporting information can be found online in the Supporting Information section.

Supporting Information S1: jcc570012-sup-0001-suppl-data.docx.